

Droplet formation behavior in a microfluidic device fabricated by hydrogel molding

Takahiro Odera · Hirotada Hiramama · Jo Kuroda ·
Hiroyuki Moriguchi · Toru Torii

Received: 9 June 2013 / Accepted: 24 December 2013 / Published online: 5 January 2014
© Springer-Verlag Berlin Heidelberg 2014

Abstract We describe the behavior of droplet formation within 3D cross-junctions and 2D T-junctions with various cross-sectional geometries that were manually fabricated using the hydrogel-molding method. The method utilizes wire-shaped hydrogels as molds to construct 3D and 2D microchannel structures. We investigated the flow patterns and droplet formation within the microchannels of these microfluidic devices. Despite being fabricated manually, the microchannels with 3D cross-junctions and 2D T-junctions were reproducible and formed highly monodispersed droplets. Additionally, the sizes of the droplets formed within the microchannels could be predicted using an experimental formula. This technique of droplet formation involves the use of a device fabricated by hydrogel molding. This method is expected to facilitate studies on droplet microfluidics and promote the use of droplet-based lab-on-a-chip technologies for various applications.

Keywords Droplet microfluidics · 3D microchannel · Agarose gel · Lithography free · Polydimethylsiloxane

1 Introduction

Droplet microfluidics has been studied for many decades (Kawakatsu et al. 1996), and numerous droplet formation methods, including the use of T-junctions (Thorsen et al. 2001; Nisisako et al. 2002; Okushima et al. 2004), flow-focusing (Anna et al. 2003; Utada et al. 2005; Nie et al.

2005), and electrostatic manipulation (Choi et al. 2007), have been developed for various applications, such as particle synthesis (Nisisako et al. 2004, 2012; Zhang et al. 2012; Hiramama et al. 2013; Aketagawa et al. 2013; Mulu-neh and Issadore 2013) and theoretical studies of droplet formation in microchannels of various configurations (Kobayashi et al. 2004a; Samie et al. 2013). Droplets form because of a balance between the interfacial tension and shear forces that are caused by the branched microchannels in microfluidic devices and the drop in pressure (Garstecki et al. 2006). Because droplet formation in a microchannel is subject to the effects of the microchannel's cross-sectional shape, droplet formation using microchannels with different shapes has been investigated in detail (Kobayashi et al. 2002, 2004a, b). Polydimethylsiloxane (PDMS) microfluidic devices have previously been fabricated to form droplets using photolithography, which is a cost-effective and rapid prototyping technology (Sollier et al. 2011). However, photolithography requires specialized facilities, such as a clean room with photolithography equipment. A rapid, non-photolithographic prototyping method would contribute to the advancement of microfluidics research in a variety of fields.

We previously reported a lithography-free, rapid prototyping method in which a hydrogel mold was used to fabricate microchannels (Hiramama et al. 2012). This method allows for the rapid fabrication of flexible 2D and 3D microchannels without requiring photolithography because hydrogel molds can be easily prepared in either glass capillaries or polytetrafluoroethylene (PTFE) tubes. We previously presented this convenient fabrication method for the rapid prototyping of microchannel devices. However, despite this convenience, the fabricated devices, specifically microchannels with triangular cross sections or

T. Odera · H. Hiramama (✉) · J. Kuroda · H. Moriguchi · T. Torii
Department of Human and Engineered Environmental Studies,
Graduate School of Frontier Sciences, The University of Tokyo,
5-1-5, Kashiwanoha, Kashiwa-shi, Chiba 277-8563, Japan
e-mail: hhirama@dt.k.u-tokyo.ac.jp

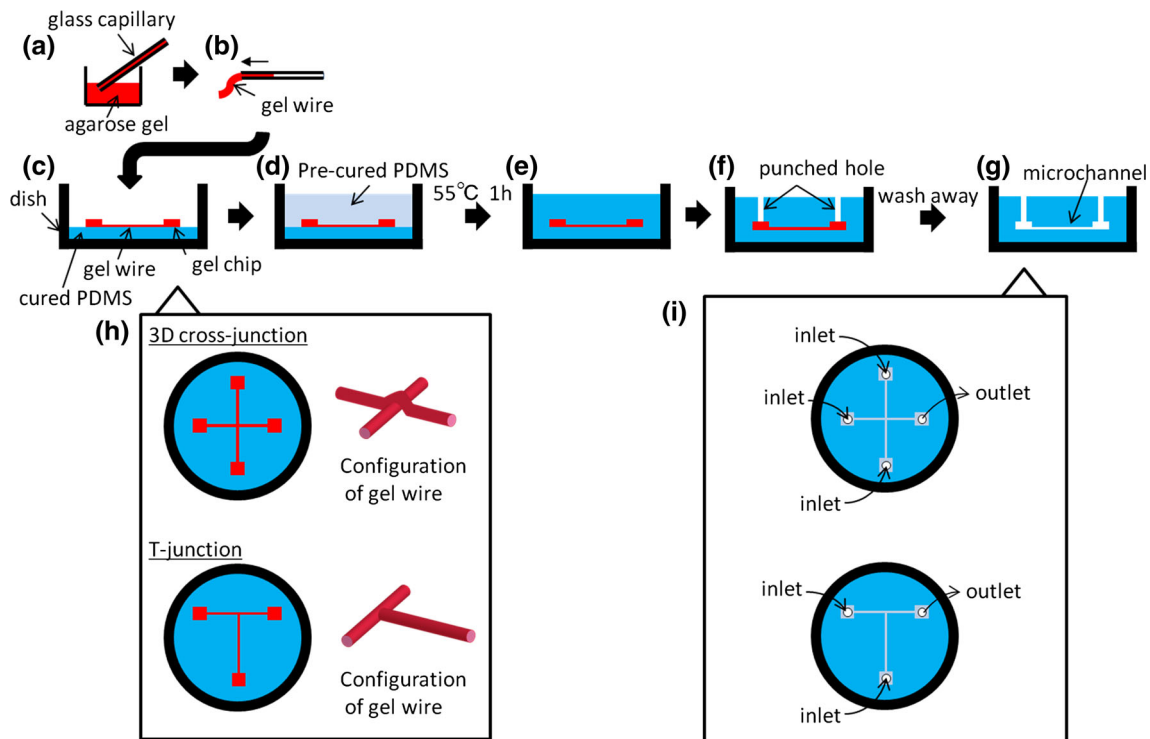


Fig. 1 Fabrication process of a PDMS microfluidic device using the hydrogel-molding method. **a** Agarose gels are inserted into glass capillaries. **b** Agarose gels are cured and ejected from the capillary. **c** Gel wires and gel chips are arranged on pre-cured PDMS sheets according to the desired channel design. **d** Pre-cured PDMS is poured

into the dish. **e** PDMS is cured by heating. **f** Holes are punched into gel chips. **g** Excess agarose gel is washed away. **h** Microchannel configuration. **i** Design of inlet and outlets for fluid injection and ejection

3D cross-junctions, have not been studied with respect to droplet microfluidics. The fabrication of microchannels with a triangular cross section is crucial to facilitating droplet formation and that of microchannels with 3D cross-junctions is crucial to the mass production of Janus droplets or particles (Muluneh and Issadore 2013).

In this study, we investigated droplet formation behavior within several types of microchannels (i.e., 2D channels, 3D channels, and channels with various cross-sectional geometries) fabricated by the abovementioned method to expand the device's applications, and we report the effect of these architectures on the formation of microdroplets and experimental formulae for predicting the sizes of the formed droplets.

2 Materials and methods

2.1 2D microchannel fabrication

The fabrication process, which is the same process used in our previously reported method involving hydrogel molds (Hirama et al. 2012), is shown in Fig. 1. Briefly, an aqueous solution of 16 % (v/v) glycerol, 3 % (w/v) agarose

(Agarose L, Wako, Japan), and 0.05 % (w/v) food dye (Red No. 102, Tokyo Chemical Industry, Japan) was prepared and cured in a glass capillary to form a gel wire. The diameter of the gel wire determined the size of the microchannel (Fig. 1a, b). Gel wires were then arranged into the desired channel design on pre-cured PDMS (10:1 weight ratio of base resin to curing agent; SILPOT 184, Dow Corning, Japan). A 60-mm dish (60 mm × 15 mm, Fisher Scientific, USA) was used to contain the embedded PDMS. An additional layer of PDMS pre-polymer was cast onto the pre-cured PDMS and agarose gel wires (Fig. 1c, d), and the PDMS was cured at 55 °C, which is below the melting point of agarose, for 1 h. After curing, a biopsy punch was used to create holes in the PDMS device, and boiling water was flushed through the microchannels to remove excess agarose gel (Fig. 1e, f). Finally, the microchannels were treated with Sigmacote (Sigma, USA) to render them hydrophobic.

2.2 Fabrication of 3D microchannel cross-junctions

A 3D microchannel cross-junction was generated by crossing one gel wire over a second gel wire (Figs. 1h, top, 2a). Glass capillaries with inner diameters of 300 μm

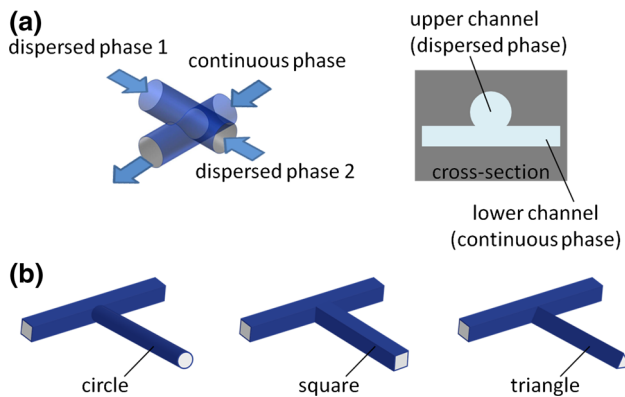


Fig. 2 Schematic drawing of microchannel configuration. **a** A 3D microchannel cross-junction as viewed from above (*left*) and along its cross section (*right*). **b** A microchannel T-junction with different cross-sectional geometries. In each device, one microchannel has a square cross-sectional area and the other microchannel has either a circular, square, or triangular cross-sectional area

(special order, Sun-yell Co., Japan) and 600 μm (G-1, Narishige, Japan) and PTFE tubes with inner diameters of 800 μm (Flon Ind. Co., Japan) were used to fabricate gel wires and 3D microchannel cross-junction devices.

2.3 2D microchannel T-junctions with various cross-sectional geometries

The microchannel structure ultimately depends on the cross-sectional area of the glass capillary used to prepare the gel wire. In this study, glass capillaries with circular, square, or triangular cross sections (special order, Takao Manufacturing Co., Japan) were used to prepare gel wires for microchannels that would contain dispersed-phase solutions. Capillaries with a square cross-sectional area were used to prepare microchannels containing continuous phase solutions (Fig. 2b).

2.4 Microchannel droplet formation

2.4.1 3D microchannels

Mineral oil (Sigma, USA) supplemented with 1 % (w/w) surfactant (SY glyster CRS-75; Sakamoto Chemical Ind., Japan) with a viscosity of 21.5 mPa·s was used as the continuous phase. A solution of 1 % (w/w) food coloring (Red 102 or Blue 1, Tokyo Chemical Industry, Japan) in either deionized (DI) water or 2 % (w/v) methylcellulose was used as the dispersed phase; the viscosities of the solutions were 1.29 and 21.6 mPa·s, respectively. The interfacial tensions between the dispersed and continuous phase (mineral oil) were 8.96 and 13.97 mN m⁻¹ for the DI water and methylcellulose solutions, respectively.

Table 1 Experimental conditions used to investigate flow patterns with 3D microchannel cross-junctions

	Diameter of microchannel	Continuous phase	Dispersed phase (viscosity [mPa·s])
Condition 1	φ250 μm	Mineral oil	DI water (1.29)
Condition 2	φ500 μm	Mineral oil	DI water (1.29)
Condition 3	φ500 μm	Mineral oil	Methylcellulose (aq.) (21.6)

Table 2 Experimental conditions used to measure the diameters of biphasic droplets

Diameter of the microchannel	Flow rate of the continuous phase (ml/h) (interval)	Flow rate of the dispersed phase (ml/h)
φ250 μm	0.1–1.0 (0.1)	0.2
	0.1–1.0 (0.1)	0.4
	1.0–10.0 (1.0)	1.0
φ500 μm	0.4–4.0 (0.4)	0.2
	0.4–4.0 (0.4)	0.4
φ750 μm	1.0–10.0 (1.0)	1.0
	2.0–20.0 (2.0)	2.0
	2.0–20.0 (2.0)	4.0

We used the 3D microchannel cross-junctions to detect the flow patterns of the dispersed and continuous phases and observe droplet formation. This geometry was achieved by varying the diameter of the microchannel as well as the physical properties and flow rates of the fluid, as shown in Table 1. The continuous phase flowed in the lower channel, and the dispersed phase flowed in the upper channel (Fig. 2a). Using DI water with food coloring as the dispersed phase, we measured the biphasic droplet diameter with varying flow rates and channel diameters, as shown in Table 2. The flow rate of the continuous phase was fixed, and the dispersed phase was varied at a constant rate. For each condition, 50 droplets were measured.

2.4.2 2D microchannels

We measured the diameter of droplets formed in microchannel T-junctions with different cross-sectional geometries by adjusting the flow rate of the dispersed phase to 0.4 ml h⁻¹ (0.4–4.0 ml h⁻¹), 0.8 ml h⁻¹ (0.4–4.0 ml h⁻¹), and 2.0 ml h⁻¹ (1.0–10.0 ml h⁻¹). The values in parentheses represent the flow rate of the continuous phase. DI water with food coloring was used as the dispersed phase. The flow rate of the dispersed phase was fixed, and the flow rate of the continuous phase was varied at a constant rate. For each condition, 50 droplets were analyzed.

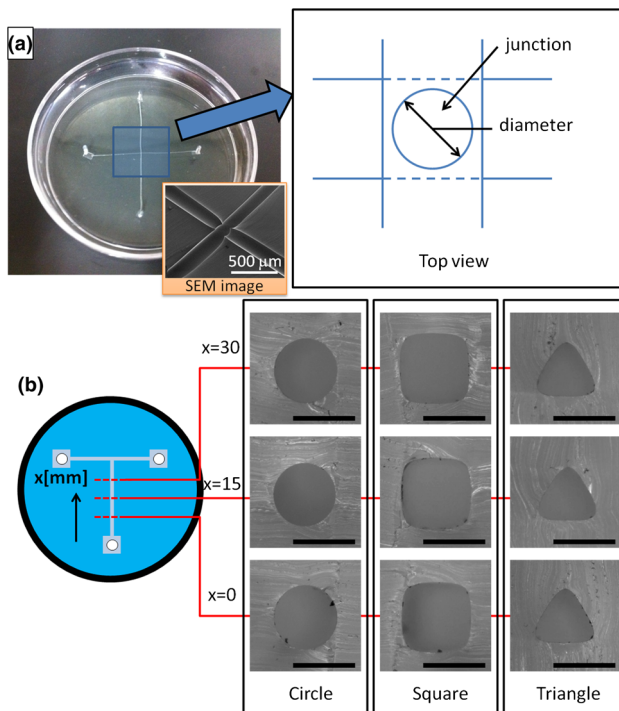


Fig. 3 Dimensions of fabricated devices. **a** Diameter of fabricated 3D cross-junctions. For the 3D microchannels, the junction was approximated by a circle. **b** The cross-sectional geometry of microchannel T-junctions. Uniform cross sections were observed at each position. The scale bars are 500 μm

Table 3 Cross-sectional areas of microchannel T-junctions with different geometries (corresponding to Fig. 3b)

X (mm)	Cross-sectional area (mm^2)		
	Circle	Square	Triangle
0.0	0.175	0.241	0.121
7.5	0.172	0.246	0.119
15.0	0.168	0.244	0.119
22.5	0.172	0.242	0.114
30.0	0.173	0.244	0.120
Average	0.172	0.244	0.119
Standard deviation	0.003	0.002	0.003
CV (%)	1.48	0.76	2.27

3 Results and discussion

3.1 Microchannel fabrication

The diameters of the 3D cross-junctions were measured by filling the microchannels with colored water and examining them under a microscope (Fig. 3a). These diameters were determined to be 245 μm (9 μm) in 250- μm microchannels, 497 μm (10 μm) in 500- μm microchannels, and 743 μm (3 μm) in 750- μm microchannels, with the

standard deviation (SD) shown in parentheses. The number of prepared and measured junctions was 5 each. The acute junction angle in the 2D microchannel T-junctions was 87° (4.6°), with the SD shown in parentheses. The number of prepared and measured junctions was 15 each. The coefficients of variation (CV) in both the diameter and the angle were less than approximately 5 %, which indicates that the hydrogel-based method yielded reproducible microchannels. Table 3 lists the cross-sectional areas of microchannel T-junctions with various geometries (measured as shown in Fig. 3b). The results confirm that the hydrogel-based fabrication method generated uniform microchannels (Fig. 4).

3.2 Flow patterns in 3D cross-junctions

We investigated specific flow patterns in 3D microchannel cross-junctions. In this study, the flow pattern in 2D devices was not investigated because it has already been widely studied (Thorsen et al. 2001; Nisisako et al. 2002; Garstecki et al. 2006). The flow patterns and types of droplets formed are shown in Fig. 5. Lee et al. (2009) previously reported that microfluidic flow is controlled by the balance of viscous stresses (described as viscosity) and capillary pressure (described as the capillary number). In their study, the flow rate was expressed as the capillary number $Ca = \eta U / \sigma$, where η is the viscosity, σ is the interfacial tension, and U is the flow velocity.

The biphasic flow and biphasic droplet formation of an immiscible two-layer flow were stable, as shown in Fig. 5. However, alternating droplet generation, which denotes the formation of two types of droplets (red- and green-colored droplets), resulted in unstable phenomena. The flow conditions “unstable (biphasic flow),” “unstable (biphasic droplet),” “unstable (alternating droplet generation),” and “unstable” indicate flow patterns that transformed into another flow pattern within 5 min. Biphasic droplet generation in the 3D cross-junctions was observed for capillary numbers within the following ranges: $2 \times 10^{-4} < Ca_C < 1 \times 10^{-1}$ and $3 \times 10^{-5} < Ca_d < 6 \times 10^{-4}$, where Ca_C and Ca_d are the capillary numbers of the continuous and dispersed phases, respectively. Therefore, monodispersed biphasic droplets were expected to form in these capillary number ranges irrespective of the microchannel diameter or the physical properties of the fluids.

Alternating droplet generation was only observed when the junction was filled with mineral oil (continuous phase) prior to the addition of water (dispersed phase). The process in which monodispersed droplets were alternatively generated for more than 5 min was classified as monodispersed alternating droplet generation. The other instances were classified as unstable alternating droplet generation. Unstable alternating droplet generation was observed in wider channel devices ($\phi 500 \mu\text{m}$; conditions 2 and 3 in

Fig. 4 Microchannel T-junctions with different cross-sectional geometries. **a** Photograph of gel wires with square and triangular cross sections. **b** Micrographs of T-junction cross sections obtained by phase contrast (*top*) and electron microscopy (*bottom*). The scale bars are 500 μm

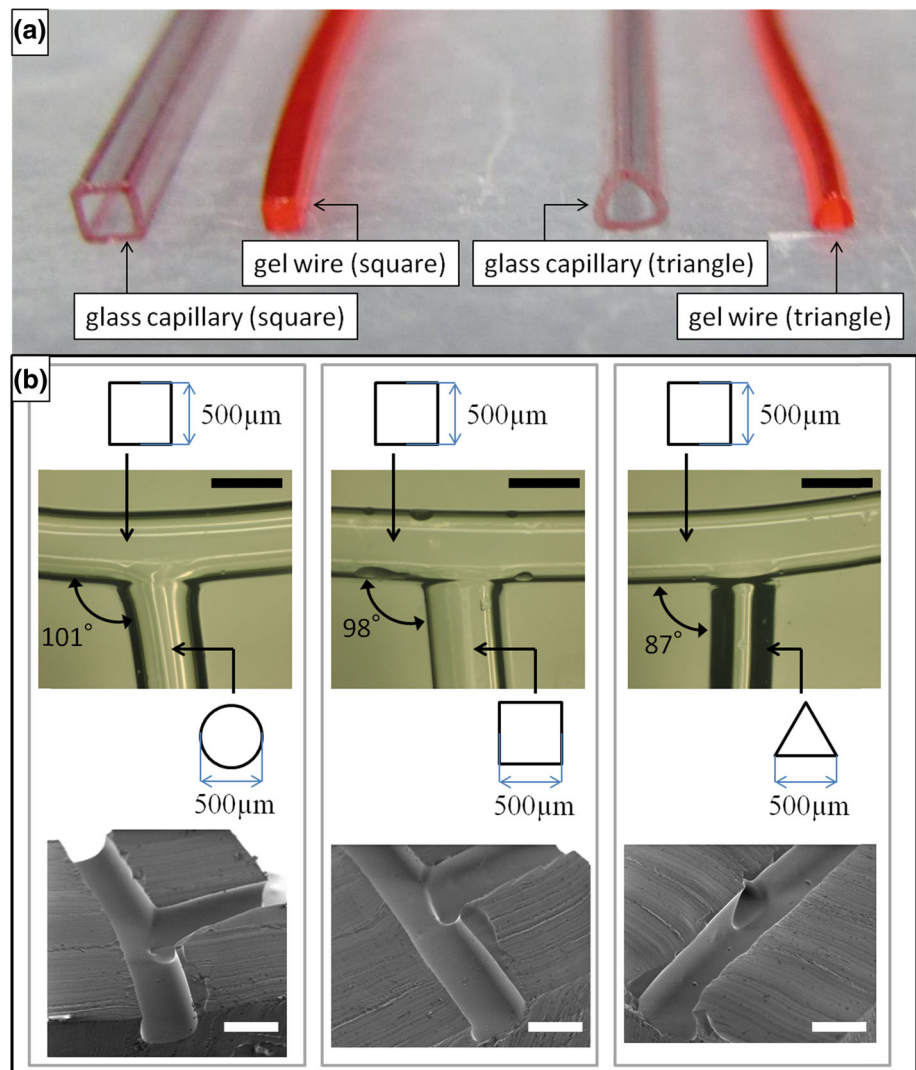


Table 1), and monodispersed generation was observed only in wider channel devices using the dispersed phase with a lower viscosity (DI water; condition 2 in Table 2). In addition, alternating droplet generation was observed within the range of $10^{-3} < Ca_c < 10^{-2}$. The droplet formation behavior in 3D microchannel devices has not been previously studied, and thus, the data obtained in this study cannot be directly compared with other data published in previous reports. However, we compared the obtained Ca range to previously reported data for 2D alternating droplet generation by assuming the 3D device acted as a 2D cross-junction device. The Ca range was observed to be within previously reported Ca ranges for alternating droplet generation, and the behavior of alternating droplet generation with the devices fabricated by hydrogel molding agreed with the results reported in previous studies (Zheng et al. 2004; Lee et al. 2010).

Figure 6 shows the relationship between the droplet diameter and the capillary number ratio, which is defined

as $A = Ca_d/Ca_c$, where Ca_d and Ca_c are the capillary numbers of the dispersed and continuous phases, respectively. In this study, the figures were created by using the dimensionless diameter to describe the formed droplet size on a relative scale between the droplet and microchannel dimensions. The dimensionless diameter, d_{nd} , is equal to the mean diameter of the droplets, d_m , divided by the hydraulic diameter of the microchannel, defined as $d_h = 4S/L$, where S is the cross-sectional area of the microchannel and L is the circumference of the channel. In this figure, the dimensionless diameter of a droplet formed via 3D cross-junctions with channel diameter D (μm) is represented as $d_{nd} = k_D A^{l_D}$, where k_D and l_D are constants. The correlation coefficients for the three experimental conditions exceeded 0.9; therefore, the droplet diameter could be accurately estimated from this expression. The relationship between the flow rate of the dispersed phase and droplet size in 3D microchannel devices has not been previously studied; therefore, the data

Fig. 5 Flow pattern and droplet formation in 3D cross-junctions. The “biphasic flow” and “biphasic droplets” consisted of a two-layer immiscible flow. “Alternating droplet generation” produced alternating monodispersed droplets. These flow patterns persisted for more than 5 min. By contrast, the flow conditions “unstable (biphasic flow),” “unstable (biphasic droplet),” “unstable (alternating droplet generation),” and “unstable” were flow patterns that transformed into another flow pattern within 5 min. In the “unstable (transient)” flow condition, biphasic flow and biphasic droplet formation were unstable and alternated. Circles indicate measurement points

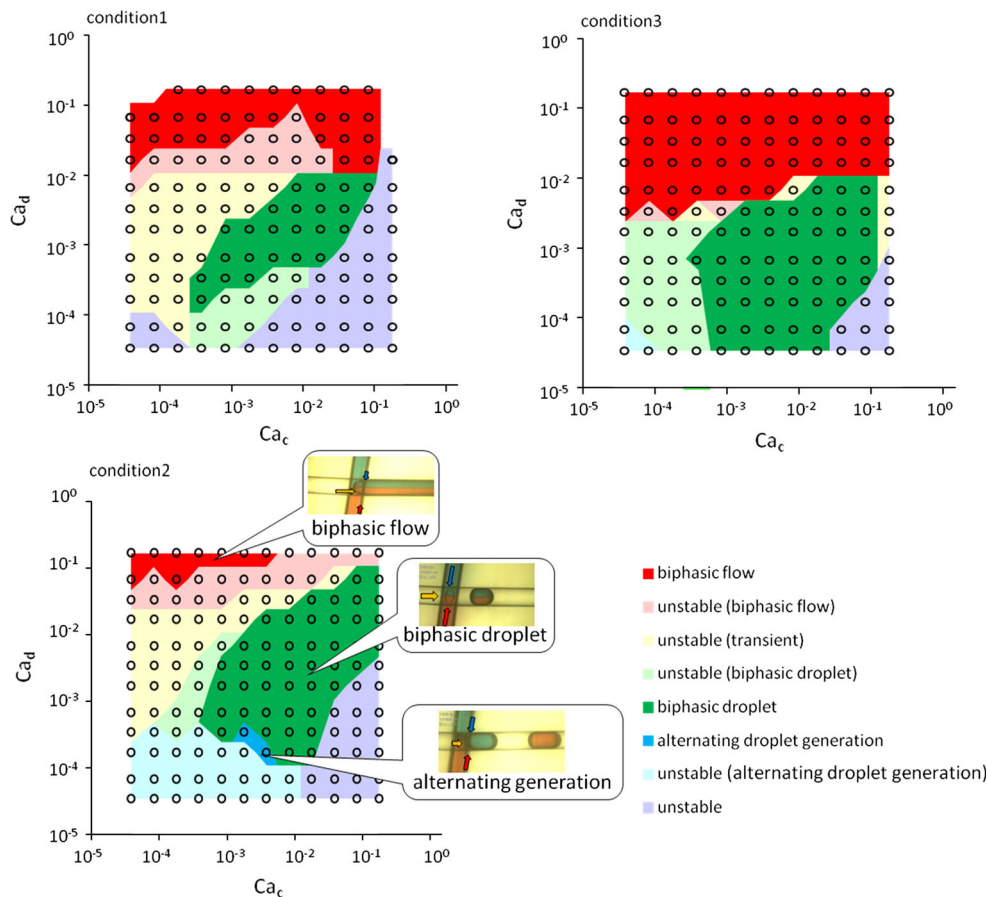
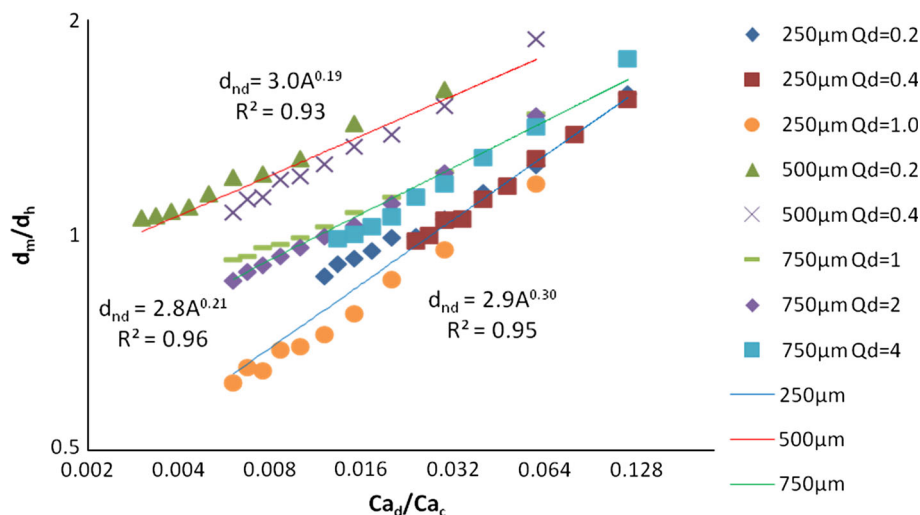


Fig. 6 Relationship between the dimensionless droplet diameter and capillary number ratio of 3D microchannel cross-junctions. The hydraulic diameters of the 250-, 500-, and 750- μm microchannels were 250, 500, and 750 μm , respectively. Q_d shows the flow rates of dispersed phase (ml/h). The coefficient of variation (CV) in the droplet diameters at each point was less than 5%. The graph shows log–log plots. The fits were obtained from the experimental results



obtained in this study cannot be directly compared with other data from previous reports. However, we compared the obtained relationship between the flow rate of the dispersed phase and droplet size to previously reported data obtained from 2D cross-junction devices by assuming that the 3D devices acted as 2D cross-junction devices

based on the data shown in Fig. 6. In the 3D device, the droplet sizes were proportional to the flow rates of the dispersed phase, and the proportionality constants were 0.95–3.0. This result is very similar to previously published experimental results, which indicate values of 1–2.52 (Xu et al. 2008).

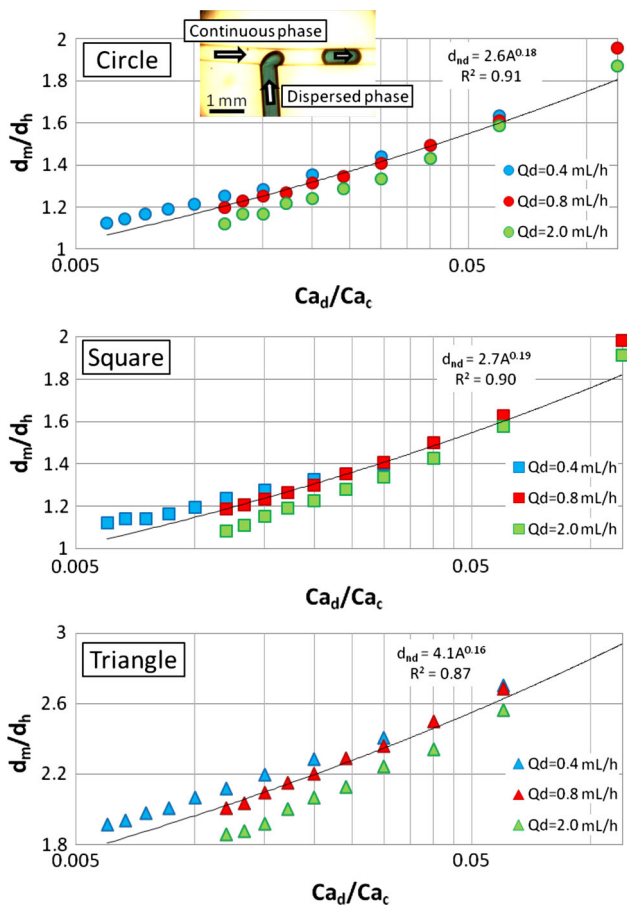


Fig. 7 Relationship between the dimensionless droplet diameter and capillary number ratio in microchannel T-junctions. Each graph shows the results from microchannel devices with different cross-sectional geometries for the dispersed phase. The hydraulic diameters of the circular, square, and triangular cross-sectional microchannel were 500, 500, and 289 μm , respectively. Q_d shows the flow rates of dispersed phase. The graphs show lin-log plots. The fits were determined from experimental results

3.3 Droplet formation in T-junctions with different cross-sectional geometries

Figure 7 shows the relationship between the droplet diameter and the ratio of capillary numbers, $A = Ca_d/Ca_c$, in T-junctions with different cross-sectional geometries. In these 2D T-junctions, the dimensionless diameter, d_n , can also be accurately expressed as $d_{nd} = k_D A^{1D}$. Additionally, the droplet size was proportional to the flow rate of the dispersed phase in T-junction microchannels with a square cross section, and the proportionality constant was 1.7. This result is very similar to previously published experimental and simulation results, which have indicated values of 1 (Garstecki et al. 2006) and 1.82 (Liu and Zhang 2009) for this constant. Therefore, the device presented herein was confirmed to be a reliable rapid prototyping microfluidic device for various applications.

The diameters of the droplets were similar in T-junctions with circular and square cross sections; however, these diameters were smaller than those of T-junctions with triangular cross-sectional microchannels (Fig. 7). The variation in droplet size was effected by the difference in channel depth; the circular and square cross-sectional depths were approximately 500 μm , and the triangular cross-sectional depth was approximately 430 μm . According to a previous study (Chan et al. 2005), the rapid increase in channel depth at a step of a microchannel causes a sudden decrease in flow velocity, and a non-uniform Laplace pressure occurs at the corner of a junction with a step structure, which then forms and pinches the “neck” of the dispersed phase and ultimately generates droplets (Stone et al. 1986; Sugiura et al. 2001). These additional factors caused by the step structure of the triangular cross section gave rise to the difference in droplet size observed between the circular and square cross-sectional devices and the triangular cross-sectional device. Although the angle of the T-junction can also affect droplet formation, this effect was virtually negligible in this study. This observation was made because according to a previously reported study, angles within a range of 60°–120° are not affected by the resulting droplet sizes (Yeom and Lee 2011), and the junction angle in the device used in this study was approximately 90°.

The droplets formed in microfluidic devices fabricated by the hydrogel-molding method were highly monodisperse with a CV < 5 %, as previously reported (Okushima et al. 2004). This fabrication method produced devices that were equally effective in forming uniform droplets compared to existing microfluidic devices.

4 Conclusions

A hydrogel-molding method was used to fabricate 3D microchannel cross-junctions and T-junctions with various cross-sectional geometries. The fabricated microchannels containing both 3D cross-junctions and 2D T-junctions were reproducible and uniform, and they were used to evaluate microchannel flow patterns. Monodisperse biphasic droplets could be generated when the capillary numbers fell in the following ranges: $2 \times 10^{-4} < Ca_c < 1 \times 10^{-1}$ and $3 \times 10^{-5} < Ca_d < 6 \times 10^{-4}$. The dimensionless diameter of the droplets formed in 3D cross-junctions and T-junctions increased exponentially with the capillary number ratio of the continuous and dispersed phases. The diameters of the droplets formed in microchannel T-junctions with various cross-sectional geometries were compared. Microfluidic devices fabricated by hydrogel molding were used to develop a technique for droplet formation. Our results are similar to those of

previous studies; therefore, the devices fabricated in this study can be used to prototype microfluidic devices reliably and rapidly. This technique is expected to facilitate studies on droplet microfluidics and promote the use of droplet-based lab-on-a-chip technologies for various applications.

References

- Aketagawa K, Hiram H, Torii T (2013) Hyper-miniaturisation of monodisperse janus hydrogel beads with magnetic anisotropy based on coagulation of Fe₃O₄ nanoparticles. *J Mater Sci Chem Eng* 1(2):1–5. doi:10.4236/msce.2013.12001
- Anna SL, Bontoux N, Stone HA (2003) Formation of dispersions using “flow focusing” in microchannels. *Appl Phys Lett* 82(3):364. doi:10.1063/1.1537519
- Chan EM, Alivisatos AP, Mathies RA (2005) High-temperature microfluidic synthesis of CdSe nanocrystals in nanoliter droplets. *J Am Chem Soc* 127(40):13854–13861. doi:10.1021/Ja051381p
- Choi WK, Lebrasseur E, Al-Haq MI, Tsuchiya H, Torii T, Yamazaki H, Shinohara E, Higuchi T (2007) Nano-liter size droplet dispenser using electrostatic manipulation technique. *Sens Actuator A-Phys* 136(1):484–490. doi:10.1016/j.sna.2006.12.028
- Garstecki P, Fuerstman MJ, Stone HA, Whitesides GM (2006) Formation of droplets and bubbles in a microfluidic T-junction—scaling and mechanism of break-up. *Lab Chip* 6(3):437–446. doi:10.1039/B510841a
- Hirama H, Odera T, Torii T, Moriguchi H (2012) A lithography-free procedure for fabricating three-dimensional microchannels using hydrogel molds. *Biomed Microdevices* 14(4):689–697. doi:10.1007/s10544-012-9649-4
- Hirama H, Kambe T, Aketagawa K, Ota T, Moriguchi H, Torii T (2013) Hyper alginate gel microbead formation by molecular diffusion at the hydrogel/droplet interface. *Langmuir* 29(2):519–524. doi:10.1021/la303827u
- Kawakatsu T, Kikuchi Y, Nakajima M (1996) Visualization of microfiltration phenomena using microscope video system and silicon microchannels. *J Chem Eng Jpn* 29(2):399–401
- Kobayashi I, Nakajima M, Chun K, Kikuchi Y, Fukita H (2002) Silicon array of elongated through-holes for monodisperse emulsion droplets. *AIChE J* 48(8):1639–1644. doi:10.1002/aic.690480807
- Kobayashi I, Mukataka S, Nakajima M (2004a) CFD simulation and analysis of emulsion droplet formation from straight-through microchannels. *Langmuir* 20(22):9868–9877. doi:10.1021/La0487489
- Kobayashi I, Mukataka S, Nakajima M (2004b) Effect of slot aspect ratio on droplet formation from silicon straight-through microchannels. *J Colloid Interface Sci* 279(1):277–280. doi:10.1016/j.jcis.2004.06.028
- Lee W, Walker LM, Anna SL (2009) Role of geometry and fluid properties in droplet and thread formation processes in planar flow focusing. *Phys Fluids*. doi:10.1063/1.3081407
- Lee M, Park W, Chung C, Lim J, Kwon S, Ahn KH, Lee SJ, Char K (2010) Multilayer deposition on patterned posts using alternating polyelectrolyte droplets in a microfluidic device. *Lab Chip* 10(9):1160–1166. doi:10.1039/B919753b
- Liu HH, Zhang YH (2009) Droplet formation in a T-shaped microfluidic junction. *J Appl Phys*. doi:10.1063/1.3187831
- Muluneh M, Issadore D (2013) Hybrid soft-lithography/laser machined microchips for the parallel generation of droplets. *Lab Chip*. doi:10.1039/c3lc50979f
- Nie ZH, Xu SQ, Seo M, Lewis PC, Kumacheva E (2005) Polymer particles with various shapes and morphologies produced in continuous microfluidic reactors. *J Am Chem Soc* 127(22):8058–8063. doi:10.1021/ja042494w
- Nisisako T, Torii T, Higuchi T (2002) Droplet formation in a microchannel network. *Lab Chip* 2(1):24–26. doi:10.1039/b108740c
- Nisisako T, Torii T, Higuchi T (2004) Novel microreactors for functional polymer beads. *Chem Eng J* 101(1–3):23–29. doi:10.1016/j.cej.2003.11.019
- Nisisako T, Ando T, Hatsuzawa T (2012) High-volume production of single and compound emulsions in a microfluidic parallelization arrangement coupled with coaxial annular world-to-chip interfaces. *Lab Chip* 12(18):3426–3435. doi:10.1039/c2lc40245a
- Okushima S, Nisisako T, Torii T, Higuchi T (2004) Controlled production of monodisperse double emulsions by two-step droplet breakup in microfluidic devices. *Langmuir* 20(23):9905–9908. doi:10.1021/la0480336
- Samie M, Salari A, Shafii MB (2013) Breakup of microdroplets in asymmetric T junctions. *Phys Rev E*. doi:10.1103/PhysRevE.87.053003
- Sollier E, Murray C, Maoddi P, Di Carlo D (2011) Rapid prototyping polymers for microfluidic devices and high pressure injections. *Lab Chip* 11(22):3752–3765. doi:10.1039/c1lc20514e
- Stone HA, Bentley BJ, Leal LG (1986) An experimental-study of transient effects in the breakup of viscous drops. *J Fluid Mech* 173:131–158. doi:10.1017/S0022112086001118
- Sugiura S, Nakajima M, Iwamoto S, Seki M (2001) Interfacial tension driven monodispersed droplet formation from microfabricated channel array. *Langmuir* 17(18):5562–5566. doi:10.1021/La010342y
- Thorsen S, Roberts RW, Arnold FH, Quake SR (2001) Dynamic pattern formation in a vesicle-generating microfluidic device. *Phys Rev Lett* 86(18):4163–4166
- Utada AS, Lorenceau E, Link DR, Kaplan PD, Stone HA, Weitz DA (2005) Monodisperse double emulsions generated from a microcapillary device. *Science* 308(5721):537–541. doi:10.1126/science.1109164
- Xu JH, Li SW, Tan J, Luo GS (2008) Correlations of droplet formation in T-junction microfluidic devices: from squeezing to dripping. *Microfluid Nanofluidics* 5(6):711–717. doi:10.1007/s10404-008-0306-4
- Yeom S, Lee SY (2011) Dependence of micro-drop generation performance on dispenser geometry. *Exp Therm Fluid Sci* 35(8):1565–1574. doi:10.1016/j.expthermflusci.2011.07.008
- Zhang J, Coulston RJ, Jones ST, Geng J, Scherman OA, Abell C (2012) One-step fabrication of supramolecular microcapsules from microfluidic droplets. *Science* 335(6069):690–694. doi:10.1126/science.1215416
- Zheng B, Tice JD, Ismagilov RF (2004) Formation of droplets of in microfluidic channels alternating composition and applications to indexing of concentrations in droplet-based assays. *Anal Chem* 76(17):4977–4982. doi:10.1021/ac0495743